Optical, Optomechanical, and Optoelectronic Design and Operational Testing of a Multi-Stage Optical Backplane Demonstration System

by

D.V. Plant, B. Robertson, H.S. Hinton[1], M.H. Ayliffe, G.C. Boisset,
D.J. Goodwill[1], D. Kabal, R. Iyer, Y. S. Liu, D.R. Rolston, M. Venditti
T.H. Szymanski, W.M. Robertson[2], and M.R. Taghizadeh[3]
Department of Electrical Engineering
McGill University
Montreal, Canada, H3A 2A7
Phone: (514) 398-2989
Fax: (514) 398-3127
email: plant@photonics.ee.mcgill.ca

[1]University of Colorado at Boulder, Boulder, Colorado
[2]Middle Tennessee State University, Murfreesboro, TN
[3]Heriot-Watt University, Edinburgh, Scotland, UK

Abstract

In this paper, we describe the optical, optomechanical, and optoelectronic design of a multi-stage optical backplane demonstration system. In addition, operational testing and performance is discussed.

Introduction

Future digital systems such as ATM switching systems and massively parallel processing computer systems will have large PCB-to-PCB (printed circuit board) connectivity requirements to support the large aggregate throughput demands being placed on such systems. Current electronic technology may not be capable of supporting both the connection densities and the bandwidths required due to limitations of multi-point electrical connections over backplane distances [1]. Two-dimensional, free-space optical interconnects represent a potential solution to the needs of these connection-intensive digital systems. When implemented at the PCB-to-PCB level in the form of an "intelligent optical backplane" [2,3], this technology is potentially capable of providing greater connectivity at higher data rates than can be supported by current or projected electronic backplanes. This is made possible in an intelligent optical backplane because of the presence of a large number of optically interconnected smart pixel arrays which control the flow of information between the PCBs. For example, it has been shown that through the use of dynamically reconfigurable smart pixel arrays, any degree K interconnection network can be embedded into an optical backplane architecture known as the "*HyperPlane*", including linear arrays, meshes, toroids, hypercubes, crossbar-based switches, and packet-based (e.g. ATM) switches [3]. The identification of critical issues in free-space intelligent optical backplanes is being pursued in the form of system demonstrator experiments [3-9]. This paper describes a system demonstrator based on the HyperPlane architecture, Hybrid-SEED smart pixel arrays, PCB level optoelectronic device packaging, a hybrid bulk optic/microoptic relay, and novel barrel/PCB optomechanics. The entire system was constructed using a standard VME electrical backplane chassis. In addition to describing the component technologies developed, this paper will describe operational testing and characterization of the demonstrator.

Smart Pixel Design

This system is designed to implement a representative portion of an ATM switching fabric based on the HyperPlane architecture. More detailed descriptions of the architectural principles are given in [3]. The 4 stage system allows for data to be brought

0-8186-7591-8/96 $5.00 © 1996 IEEE
Proceedings of MPPOI '96

off and on the backplane via Hybrid - SEED smart pixel arrays. The hybrid-SEED technology was made available through the ARPA/COOP/AT&T Hybrid SEED workshop. The smart pixels were 4 x 4 arrays with 64 optical I/O per array. They were designed to operate in a differential mode (2 transmitter (TX) and 2 receiver (RX) windows per smart pixel). The smart pixel arrays can operate in one of three modes; the transmit mode which allows for data to be clocked onto the backplane, the receive mode which allows for extraction of data from the backplane, and the transparent mode which allows data to propagate to the next node in the system. Figure 1 shows a schematic of an individual smart pixel . The smart pixel arrays are packaged at the PCB level using mother boards and daughter boards to separate the electrical and the optical layers of the system. The system control electronics reside on the mother board, and the interface between mother boards and daughter boards is via high speed ribbon connectors.

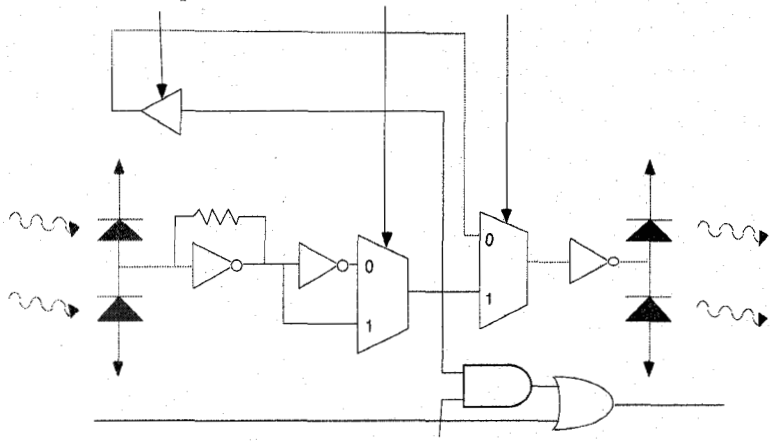

Figure 1: Smart pixel layout.

Optical Interconnect

The optical system is based on three major subassemblies and forms a unidirectional optical interconnect. Figure 2 is a schematic of the system. The first section is the optical power supply (OPS) which achieved the following specifications at the power array plane: a 8x4 spot array was created (125μm pitch in the y-direction and a 250μm pitch in the x-direction) with individual beam radiuses of 6.5μm. Each OPS consisted of a pair of doublet achromats (as the collimating lens), a quarter-wave plate (QWP), a binary phase grating (BPG), a Risley prism pair, a pair of tilt plates and a pair of doublet achromats (acting as the Fourier lenses). The Risleys prism pair and the tilt plates were included to provide lateral and angular adjustements of the output spot array. The effective focal length of the collimating and Fourier lens combination was adjusted by finely tuning the air gap separating the individual achromat. This adjustement accounted for some optical and optomechanical tolerances.

During operation, linearly polarized light enters the optical power supply (OPS) via a single mode polarisation preserving FC connectorized fiber. The fibers (corresponding to each OPS) were connected together in a tree-like configuration to a 850nm diode laser. This scalability in the optical delivery system allowed for the entire optical backplane to be driven by a single laser source. The OPS optomechanics holding the female FC receptacle provided x and y adjustements in order to allow alignment of the fiber with the mechanical axis of the OPS barrel. Each element was mounted and glued in their respective cells and subsequently inserted in a black anodized aluminum barrel. The OPS unit had an overall length of 80mm and an outside diameter of 21mm. It was designed with a long back working distance in order to allow for the insertion of a pellicle beamsplitter for illumination and imaging purposes. The pellicle beamsplitter also allowed for polarisation monitoring and power measurements of the OPS output spot array.

The daughterboard-to-daughterboard optical interconnection was achieved using a hybrid bulk/microoptic approach. Figure 3 shows a schematic of two stages in the optical interconnect system. The 8x4 spot array generated from the OPS module was relayed onto modulators at stage 1 using

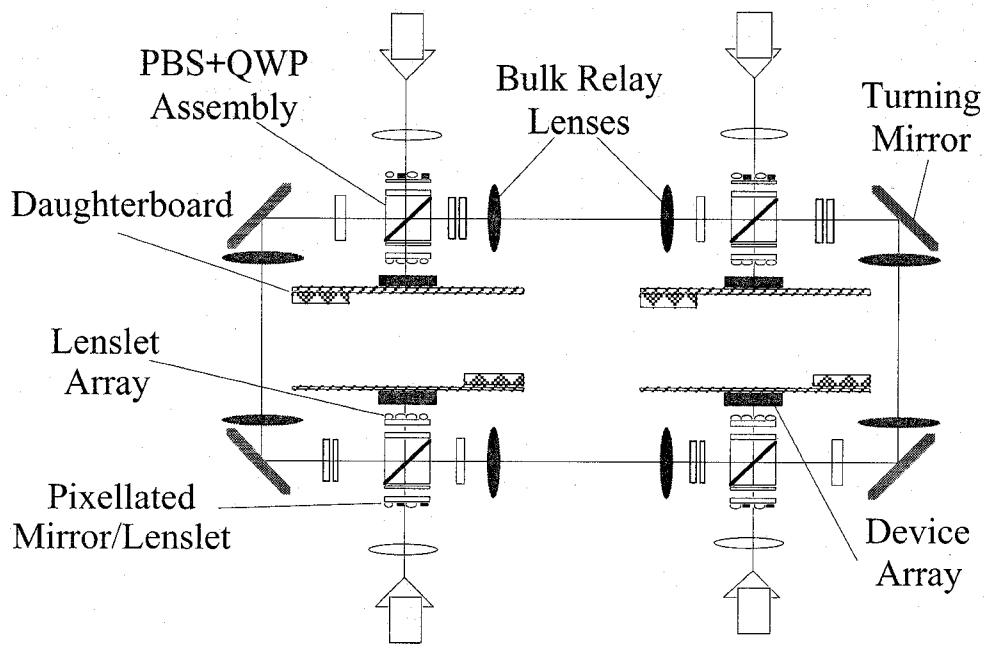

Figure 2: Optical interconnect layout.

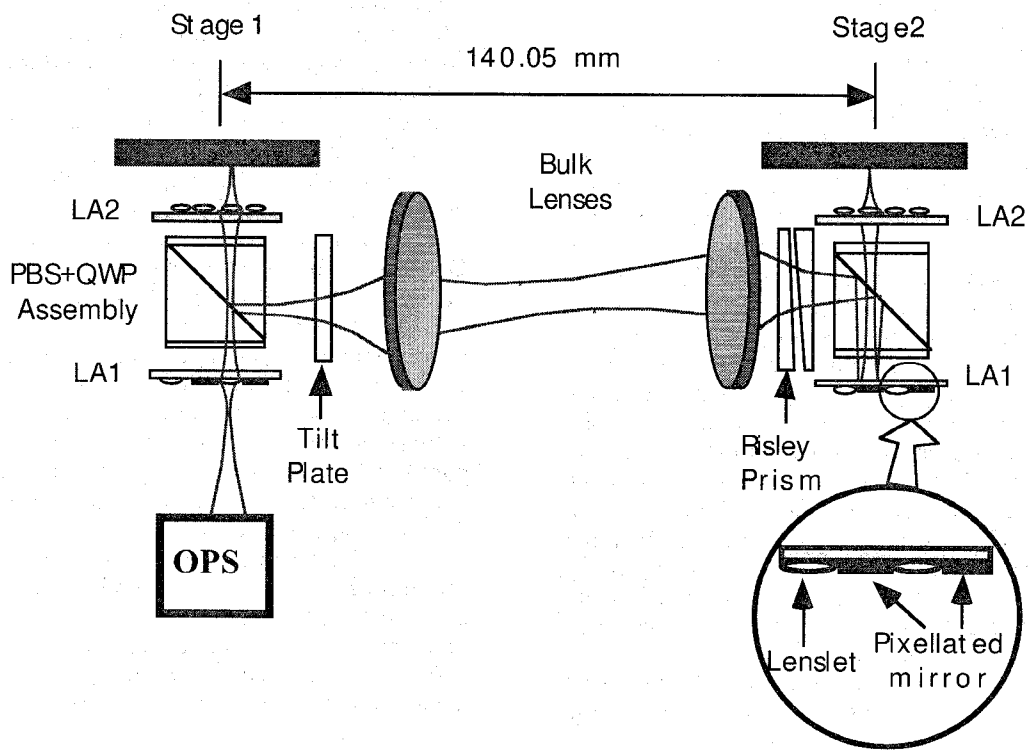

Figure 3: Hybrid bulk/microoptic interconnect

lenslet array one (LA1) and lenslet array two (LA2). These two lenslet arrays form a non-telecentric configuration. Specifically, the spot array from the OPS was located $f+z_r$ away from the LA1 and the transmitter/receiver array are located $f+z_r$ away from the LA2, respectively, where f is the focal length of the lenslet and z_r is the Rayleigh range of the beams in the spot array. This arrangement allowed for a maximum optical relay length which was required to accommodate a polarizing beamsplitter and quarter waveplate (PBS+QWP) assembly between the plane of the spot array and the plane of the smart pixel array. The PBS+QWP assembly was used to re-direct the modulated optical beams which are reflected from the transmitter array through to the bulk relay system, and then relayed to the next stage. The modulated optical beams were then reflected by a second PBS+QWP assembly at the next stage onto the pixellated mirrors. To simplify the optical system, LA1 consisted of both lenslets and pixellated mirrors. The reflected beam from the pixellated mirrors was redirected to the receiver array in the next stage. Fine adjustement was obtained by the tilt plate and Risley prism to position the spot array onto the receiver windows.

The overall optical system was optimized using Gaussian beam propagation theory. Clipping effects were taken into account during the optimization. The objective of the analysis was to get the maximum optical power into the the optical windows of the transmitter and receiver arrays. The focal lengths of the lenslets (LA1 and LA2) were chosen to be 768 μm, and the separation of the input spot array to LA1 and the plane of the smart pixel array to LA2 were 922 μm and 886 μm, respectively. The optical path length between LA1 and LA2 was 5.4 mm. The overall length of the PBS+QWP assembly was 6.7 mm. The bulk relay was achieved with two 35 mm focal length achromats. The separation between the two stages was 140 mm. This distance can be significantly reduced if bulk lenses with shorter focal length are used. This hybrid optical system was designed to be simple, compact, alignable and efficiennt.

Optomechanics

The optomechanics employed in the demonstrator were a combination of rods, barrels, and a baseplate. The objectives of these optomechanics were a) to act as a mechanical support for the optics while respecting all tolerances demanded by the optical design b) to support the packaged optoelectronics, and c) to act as an interface between a commercially available electronic chassis and the rest of the system. The system as a whole need to be rugged, scaleable and easily aligned. The optomechanics were designed to be modular in order to facilitate assembly and alignment. There were three main modules including the Optical Power Supply (OPS), the Lenslet/beamsplitter Barrel (LB), and the baseplate/bulk interconnect. In addition, numerous diagnostic features were embedded in all levels of the system. A key feature of this system is its three-dimensional nature, as is shown in Figure 4. The main bulk relay implementing the optical ring was in the xy plane (this included the baseplate), and the OPSs and hybrid relays were parallel to the z axis.

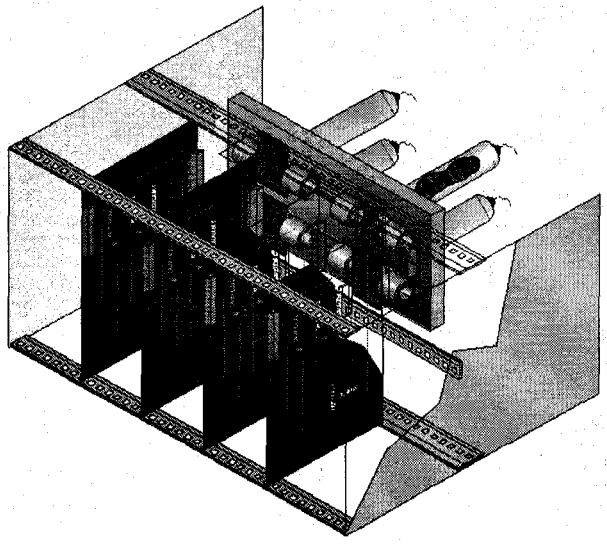

Figure 4: Schematic of system demonstrator.

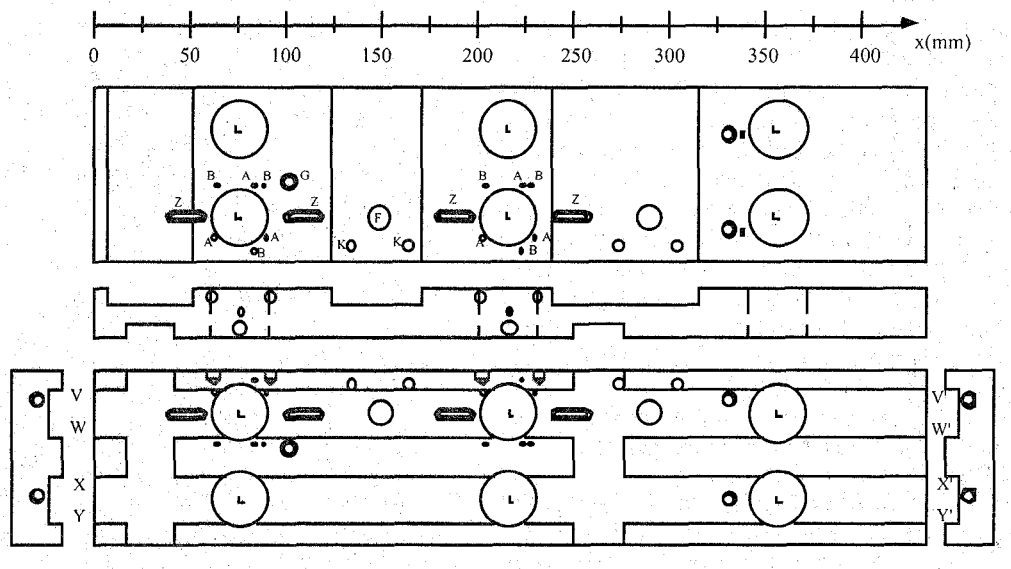

MOST HIDDEN LINES NOT SHOWN

Figure 5a:Five views of the main baseplate

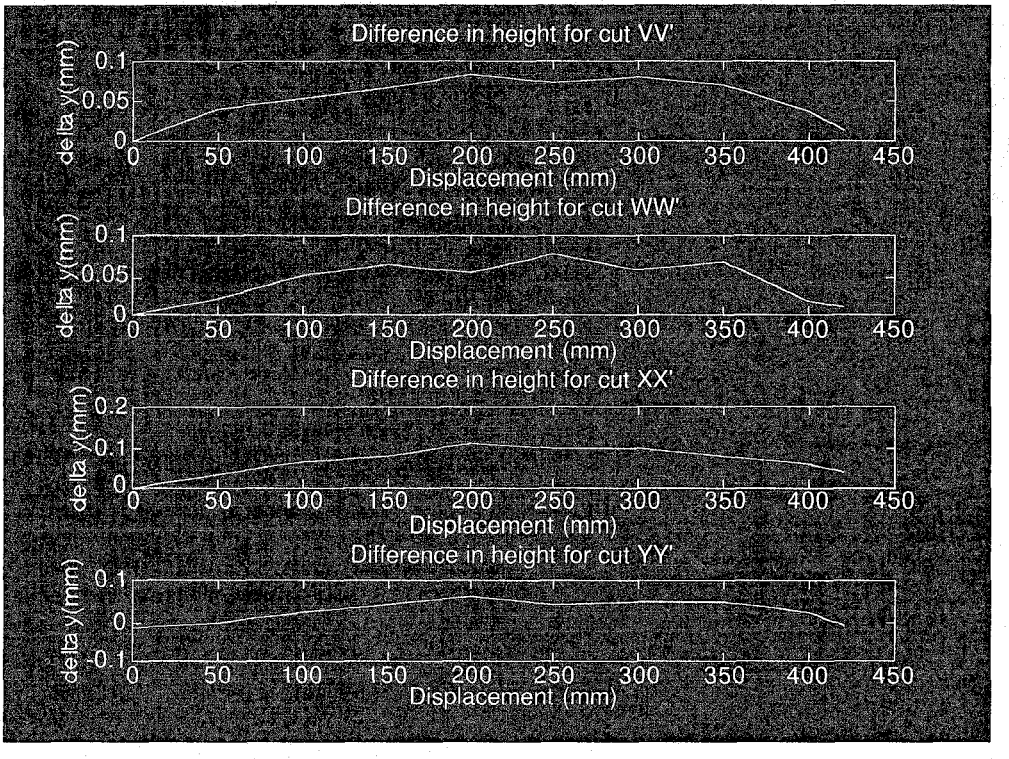

Figure 5b: measured deviations from true flat in bottom of grooves.

As in the case of the OPS, the baseplate and bulk relay made extensive use of cells and barrels to hold all the components. In order to simpify assembly and testing, all the outer diameters in the bulk relay were standardized to 25 and 30 mm. Given the severe space constraints, it was impossible to mount the bulk lenses using traditional lens mounting techniques such as retaining rings [10]. Instead, the bulk lenses were press-fit into very simple lens holders. The magnesium baseplate used in the system was 431.8 mm (17") long, was mounted vertically into the chassis, and was bolted to the side panels of the chassis. As in other similar systems [11], slots were cut into the baseplate and the component holders rested in these slots. However, given the vertical mounting and the rough handling of the system, all the bulk relay components were bolted into the baseplate since it was decided that magnetic retaining techniques would not be sufficient. Furthermore, the barrels were not in direct contact with the edges of the slots: rods were inserted in the slots and the components rested on the slots. The flatness of the baseplate was measured in the main grooves (along the x direction) along the 4 lines VV',WW', XX' and YY' as shown in Figure 5. To perform these measurements, the baseplate was rested on a granite measuring slab and a dial level indicator was passed along the grooves approximately at the place where the rods holding the bulk barrels made contact with the bottom of the groove. As can be seen, the maximum deviation was 125 μm from one end of the baseplate to the other, and is considerably less over the stretch (approx 50<x<275) where the bulk relay resides. Overall, the system optomechanics achieved the design objectives of being rugged, scaleable and providing for easy alignment of the system.

Operational Testing

The system was successfully operated with two stages optically interconnected. Currently, the system is undergoing operationally testing. Performance results will be presented. In conclusion, we have constructed a multistage optical backplane demonstration system capable of interconnecting four printed circuit boards in a unidirectional ring. This demonstration system points to the utility of using free-space digital optics to achieve PCB-to-PCB interconnection.

Acknowledgments:

This work was supported by a grant from the Canadian Institute for Telecommunications Research under the NCE program of Canada, and the Nortel/NSERC Chair in Photonic Systems. In addition, DP acknowledges support from NSERC (#OGP0155159), and FCAR (#NC-1415), TS acknowledges support from NSERC (#OGP0121601), RI acknowledge support from NSERC through a Post-Graduate Fellowship, and GB acknowledges support from FCAR through a Post-Graduate Fellowship.

References:

[1] J. W. Parker, "Optical Interconnection for Advanced Processor Systems: a review of the ESPRIT II OLIVES program," IEEE/OSA Journal of Lightwave Technology, vol. 9, no. 12, pp. 1764-1773, 1991. See also, "Optical Interconnection, Foundations and Applications," eds. C. Tocci and H.J. Caulfield, Artech House, 1994.

[2] H.S. Hinton and T.H. Szymanski, "Intelligent Optical Backplanes", *Proceedings of the Second International Conference on Massively Parallel Processing using Optical Interconnections*, IEEE Computer Society Press, pp. 133 - 143, 1995; T.H. Szymanski and H. S. Hinton, "Design of a Terabit Free-space Photonic Backplane for Parallel Computing", Ibid, pp. 16 - 27, 1995.

[3] T. H. Szymanski and H. S. Hinton, "Reconfigurable intelligent optical backplane for parallel computing and communications", Applied Optics, Vol. 32, No. 8, March 1996, pp. 1253-1268.

[4] K. Hamanaka, "Optical Bus Interconnection System Using Selfoc Lenses," Optics Letters, vol.16, no.16, pp. 1222-4, 1991.

[5] R.K. Kostuk, Yeh Jang-Hun, and M. Fink, "Distributed Optical Data Bus for Board-Level Intereonnects," Applied Optics, vol.32, no.26, pp. 5010-21, 1993.

[6] D.Z. Tsang and T.J. Goblick, "Free-Space Optical Interconnection Technology in Parallel Processing Systems," Optical Engineering, vol. 33, no. 5, pp. 1524 - 1531, 1994.

[7] D.V. Plant, B. Robertson, H.S. Hinton, W. M. Robertson, G.C. Boisset, N.H. Kim, Y. S. Liu, M.R. Otazo, D.R. Rolston, and A. Z. Shang, "An Optical Backplane Demonstrator System based on FET-SEED Smart Pixel Arrays and Diffractive Lenslet Arrays," IEEE Photon. Technol. Lett., vol. 7, No. 9, pp. 1057 - 1059, 1995.

[8] T. Sakano, T. Matsumoto, and K. Noguchi, "Three-dimensional Board-to-Board Free-Space Optical Interconnects and Their Application to the Prototype Multiprocessor System - COSINE-III," Appl. Opt., vol. 34, no. 11, pp. 1815-1822, 1995.

[9] D.V. Plant, B. Robertson, H.S. Hinton, M.H. Ayliffe, G.C. Boisset, W. Hsiao, D. Kabal, N.H. Kim,

Y.S. Liu, M.R. Otazo, D. Pavlasek, A.Z. Shang, J. Simmons, and W.M. Robertson, "A 4x4 VCSEL/MSM Optical Backplane Demonstrator System," LEOS 95, Postdeadline paper PD-2.4, 1995.
[10] P. R. Yoder, Optomechanical Systems Design, Marcel Dekker Inc., New York, 993.
[11] F. B. McCormick, T. J. Cloonan, A. L. lentine, J. M. Sasian, R. L. Morrison, M. G. Beckman, S. L. Walker, M. J. Wojcik, S. J. Hinterlong, R. J. Crisci, R. A. Novotny, and H. S. Hinton, "Five-stage free-space optical switching network with field-effect transistor self-electro-optic-effect-device smart-pixel arrays," Applied Optics Vol. 33, No. 8, pp. 1601-1618, 10 March 1994.